Redox equilibria of manganese peroxidase from *Phanerochaetes chrysosporium*: functional role of residues on the proximal side of the haem pocket

Roberto SANTUCCI*, Cristiana BONGIOVANNI*, Stefano MARINI*, Rebecca DEL CONTE†, Ming TIEN‡, Lucia BANCI† and Massimo COLETTA*[1]

*Department of Experimental Medicine and Biochemical Sciences, Università di Roma Tor Vergata, Via di Tor Vergata 135, I-00133 Roma, Italy, †Department of Chemistry and CERM, Università di Firenze, Via Luigi Sacconi 6, I-50019 Sesto Fiorentino (FI), Italy, and ‡Department of Biochemistry and Molecular Biology, Pennsylvania State University, 16802 University Park, PA, U.S.A.

Redox potentials of recombinant manganese peroxidase from *Phanerochaetes chrysosporium* have been measured by cyclic voltammetry as a function of pH, between pH 4.5 and pH 10.5. They display a bimodal behaviour (characterized by an 'alkaline' and an 'acid' transition), which indicates that (at least) two protonating groups change their pK_b values upon reduction (and/or oxidation) of the iron atom in haem. Analogous measurements have been carried out on four site-directed mutants involving residues in close proximity to the proximal ligand, His[173], in order to investigate the role played by residues of the proximal haem pocket on the redox properties of this enzyme. Results obtained suggest that the protonation state of N_δ of the proximal imidazole group is redox-linked and that it is crucial in regulating the 'alkaline' transition. On the other hand, none of the proximal mutants alters the 'acid' transition, suggesting that it is modulated by groups located in a different portion of the protein.

Key words: manganese peroxidase, proximal haem pocket, site-directed mutants, redox potentiometry, pH dependence.

INTRODUCTION

Manganese peroxidase (MnP) is a haem protein that was first discovered in the lignin-degrading fungus *Phanerochaetes chrysosporium* [1,2]. The enzyme utilizes H_2O_2 to oxidize divalent manganese [Mn(II)] to tervalent manganese [Mn(III)], which is a diffusible oxidant postulated to enter the lignin polymer [3]. Compound I oxidizes not only Mn(II) but also a variety of organic substrates [4]. On the other hand, compound II exhibits an absolute dependence on Mn(II) as a reductant [2,5].

The X-ray crystal structure of MnP has been solved [6,7] and it reveals similarity to other peroxidases, such as horseradish peroxidase (HRP), lignin peroxidase (LiP), the peroxidase from *Coprinus cinereus* (CIP) and cytochrome *c* peroxidase (YCcP) [8–12]. Most notably, residues in the distal haem pocket of MnP (i.e. His[46] and Phe[45]; the latter not present in CcP) are conserved. Also conserved is Asp[242], which is located on the proximal side of the haem pocket, forming a hydrogen-bond with N_δ of the imidazole group of the proximal His[173] residue [6]. There is an extensive debate in the literature about the role of this conserved hydrogen-bond in modulating the properties of the iron ion, and in particular its reduction potential, and consequently the reactivity of the protein [13–16]. An interesting structural aspect concerns the other residue located on the proximal side of the haem pocket near His[173], namely Phe[190], as it displays some variation among different peroxidases. This residue is phenylalanine in MnP (Phe[190]), LiP and HRP [6,9,17], tryptophan in YCcP [18] and leucine in CIP [10], and either can or cannot be hydrogen-bonded to the proximal His[173] residue. The position of this residue is close to the proximal histidine, and it suggests that it might play some role in the structural arrangement of the proximal haem pocket [6], and in particular on the orientation of the axial histidine, even though no clear evidence has been obtained for its functional role [19].

Recent studies have investigated the functional and structural properties of wild-type (wt) MnP and mutants at two residues located on the proximal side of the haem pocket, namely Asp[242] and Phe[190] [19–21]. The results suggest that these residues might play some role in modulating the function of MnP and prompted us to investigate the effect of these site-directed mutations on the redox properties and on the proton–electron coupling. Furthermore, the effect of Mn(II) on the redox properties has been investigated.

EXPERIMENTAL

Expression and purification

The mutagenesis, expression and purification of recombinant MnP were carried out as described previously [20,22]. The purified enzyme had an $R_Z \geqslant 4.5$ (A_{407}/A_{280}), and the concentration was determined using an absorption coefficient, $\epsilon = 127$ $mM^{-1} \cdot cm^{-1}$ at 407 nm [23].

Direct current (DC) cyclic voltammetry measurements

DC cyclic voltammograms were run on a pyrolytic graphite (PG) electrode coated with a polymeric film [composed of an anionic

Abbreviations used: MnP, manganese peroxidase; LiP, lignin peroxidase; YCcP, yeast cytochrome *c* peroxidase; CIP, peroxidase from *Coprinus cinereus*; TBPMC, tributylmethyl phosphonium chloride polymer; SCE, saturated calomel electrode; DC, direct current; wt, wild-type; HRP, horseradish peroxidase; PG, pyrolytic graphite.

[1] To whom correspondence should be addressed (e-mail coletta@seneca.uniroma2.it).

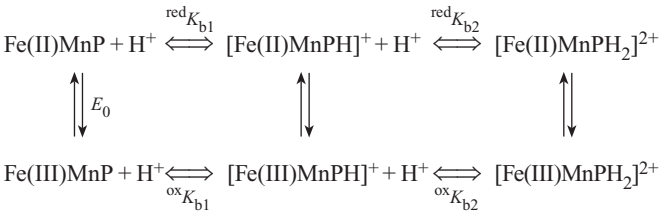

Scheme 1 Protonation scheme of the redox equilibria

exchange resin, polystyrene cross-linked with 1% (w/v) divinyl benzene, bound to a tributylmethyl phosphonium chloride (TBPMC) polymer, entrapping the protein.

Modified PG electrodes were prepared as previously described [24]. Briefly, TBMPC was dissolved in DMSO to give a 0.035% (w/v) solution; a volume of 10 μl was then mixed with 40 μl of 0.2 mM MnP/water solution and deposited (by a microsyringe) on to a PG electrode surface (2 mm diameter), previously polished using an alumina (0.3 μm particle size)/water slurry, followed by extensive sonication in deionized water. Before use the modified electrode was left to dry for 2–3 days at 5 °C.

DC cyclic voltammograms were run in degassed 100 mM acetate, phosphate or carbonate buffers, depending on the pH investigated. In the electrochemical cell, the anaerobic environment was obtained by gently flowing N_2 (high-purity grade) above the surface of the solution for approx. 20 min before measurements were taken. A PG electrode (AMEL, Milan, Italy) was the working electrode, a saturated calomel electrode (SCE; AMEL) was the reference electrode and a platinum ring was the counter-electrode. A multipolarograph Amel 433 interfaced with a personal computer as the data processor was employed for cyclic voltammetry measurements.

Data analysis

The pH-dependence of the redox potential obtained by cyclic voltammograms shows that at least two protonating groups are required to account for the observed behaviour (see Scheme 1).

The pK_b [$= \log_{10}(K_b)$] values of the controlling ionizations were calculated by fitting the data to Eqn. (1):

$$E = E_0 \cdot (1 + {}^{red}K_{b1} \cdot [H^+] + {}^{red}K_{b2} \cdot [H^+]^2) / (1 + {}^{ox}K_{b1} \cdot [H^+] + {}^{ox}K_{b2} \cdot [H^+]^2) \quad (1)$$

where E is the observed redox potential and E_0 refers to the redox potential of the unprotonated MnP. Different K_b values refer to the proton association constants for the protonating groups in the oxidized (ox) and in the reduced (red) forms.

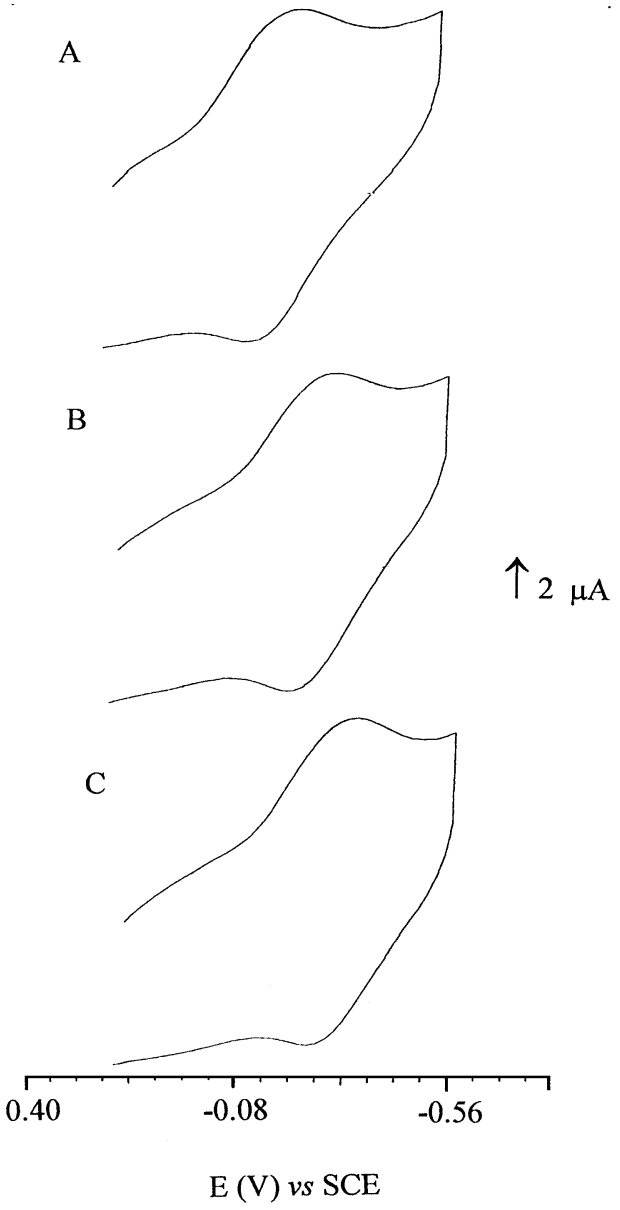

Figure 1 Cyclic voltammograms of TBMPC-embedded wt MnP at a PG electrode over the potential range between +0.4 and −0.8 V against a SCE

Cyclic voltammograms were run, at 25 °C, in 0.1 M sodium acetate buffer, pH 5.0 (**A**), and in 0.1 M sodium phosphate buffer, pH 7.0 (**B**) and pH 8.0 (**C**).

RESULTS AND DISCUSSION

Cyclic voltammetry measurements showed that in solution MnP produces no voltammetric signal at a naked PG electrode. On the other hand, rapid electron transfer is observed when the protein was embedded in a solid, inert TBMPC membrane coating the electrode (see the Experimental section). Over the whole pH range investigated (i.e. pH 4.5–10.5) the DC cyclic voltammograms of the membrane-trapped protein, dipped in the appropriate buffer, exhibited a well-defined electrochemistry for scan rates ranging between 50 and 500 mV/s. At lower scan rates the current intensity was too small to be accurately measured. Observed cathodic and anodic currents were almost identical, with an intensity ratio (i_{pa}/i_{pc}) close to unity. Such features demonstrate that the TBMPC membrane favours the direct (unmediated) electrochemistry of the protein. This explains the much sharper voltammograms obtained than those previously reported for the same protein in solution [20]. Figure 1 shows DC cyclic voltammograms for wt MnP at various pH values run at a 100 mV/s scan rate. Under the conditions investigated, the voltammetric peak current was found to depend on the square root of the scan rate, as expected for a diffusion-controlled redox process. At a scan rate of 100 mV/s, the ΔE_p values (i.e. the peak separation) were close to the theoretical value of $\Delta E_p = 57$ mV, which is expected for a one-electron-transfer reaction [25], and this was observed at all pHs investigated. At faster scan rates the

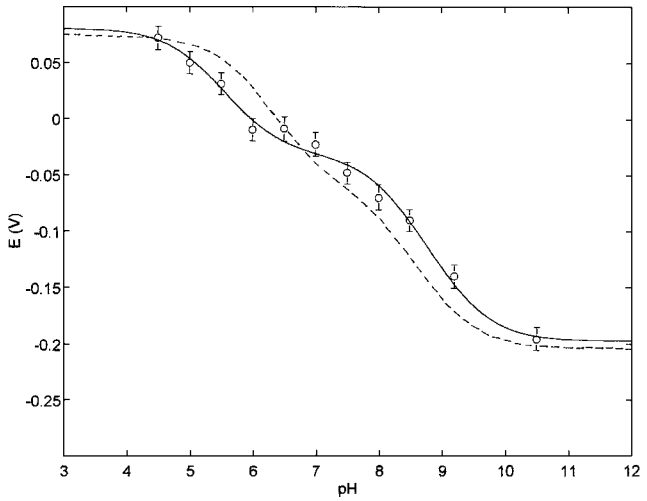

Figure 2 pH-dependence of the redox potential, *E*, for wt MnP

Experimental points are the average of multiple measurements (at least three) and the standard deviations are reported. The continuous line was obtained by applying Eqn. (1) with the parameters reported in Table 1. The dashed line corresponds to the least-squares fitting of the data according to the following equation:

$$E = E_0 \cdot {}^{red}P/{}^{ox}P$$

where ${}^{red}P = 1 + ({}^{red}K_{b1} + {}^{red}K_{b2} + {}^{red}K_{b3}) \cdot [H^+] + [{}^{red}K_{b1} \cdot ({}^{red}K_{b2} + {}^{red}K_{b3}) + {}^{red}K_{b2} \cdot {}^{red}K_{b3}] \cdot [H^+]^2 + {}^{red}K_{b1} \cdot {}^{red}K_{b2} \cdot {}^{red}K_{b3} \cdot [H^+]^3$ and ${}^{ox}P = 1 + ({}^{ox}K_{b1} + {}^{ox}K_{b2} + {}^{ox}K_{b3}) \cdot [H^+] + [{}^{ox}K_{b1} \cdot ({}^{ox}K_{b2} + {}^{ox}K_{b1}) \cdot {}^{ox}K_{b3} + {}^{ox}K_{b2} \cdot {}^{ox}K_{b3}] \cdot [H^+]^2 + {}^{ox}K_{b1} \cdot {}^{ox}K_{b2} \cdot {}^{ox}K_{b3} \cdot [H^+]^3$, fixing ${}^{ox}Ks$ to pK_a values reported previously [i.e. ${}^{ox}K_{a1} = 7.587 \times 10^{-10}$ M ($pK_a = 9.12$), ${}^{ox}K_{b1} = 1.318 \times 10^9$ M^{-1}, ${}^{ox}K_{a2} = 2.952 \times 10^{-9}$ M ($pK_a = 8.53$), ${}^{ox}K_{b2} = 3.388 \times 10^8$ M^{-1}, ${}^{ox}K_{a3} = 1.622 \times 10^{-7}$ M ($pK_a = 6.79$) and ${}^{ox}K_{b3} = 6.166 \times 10^6$ M^{-1}] [21], and leaving the other parameters floating. Parameters obtained from the fitting procedure were: ${}^{red}K_{b1} = 3.31(\pm 1.35) \times 10^8$ M^{-1} ($pK_b = 8.52 \pm 0.12$), ${}^{red}K_{b2} = 1.17(\pm 0.41) \times 10^8$ M^{-1} ($pK_b = 8.07 \pm 0.13$), ${}^{red}K_{b3} = 6.46(\pm 1.86) \times 10^5$ M^{-1} ($pK_b = 5.81 \pm 0.11$) and $E_0 = -0.201 \pm 0.025$ V. For further details see the text.

Table 1 Redox potentials and pK_b values of redox-linked groups in wt MnP and some of its mutants

pK_b was obtained by fitting the pH-dependence of the redox potential to Eqn. (1). The reported parameters were obtained by employing different buffers at different pHs, apart from one mutant where the parameters were obtained using only phosphate buffer.

	${}^{ox}pK_{b1}$	${}^{ox}pK_{b2}$	${}^{red}pK_{b1}$	${}^{red}pK_{b2}$	E_0 (V)
Wt MnP	9.39 ± 0.16	5.95 ± 0.13	8.17 ± 0.13	5.13 ± 0.11	-0.197 ± 0.023
$Asp^{242} \rightarrow Glu$	9.82 ± 0.17	5.88 ± 0.13	8.17 ± 0.12	4.87 ± 0.10	-0.270 ± 0.031
$Asp^{242} \rightarrow Ser$	8.78 ± 0.15	5.55 ± 0.12	7.43 ± 0.12	4.75 ± 0.11	-0.201 ± 0.019
$Asp^{242} \rightarrow Ser$ only phosphate	9.10 ± 0.17	6.12 ± 0.16	8.29 ± 0.14	5.44 ± 0.12	-0.136 ± 0.015
$Phe^{190} \rightarrow Val$	9.27 ± 0.17	5.73 ± 0.16	8.11 ± 0.14	4.92 ± 0.12	-0.187 ± 0.021
$Phe^{190} \rightarrow Leu$	9.34 ± 0.18	5.93 ± 0.15	7.95 ± 0.13	5.08 ± 0.13	-0.259 ± 0.028

ΔE_p increased (up to 140–150 mV for scan rates of 500 mV/s), indicating the occurrence of quasi-reversibility.

Figure 2 shows the pH-dependence of the redox potential for wt MnP, and the data at pH 7.0 agree with those already reported [23]. The data clearly showed that its redox behaviour was functionally modulated by the protonation of (at least) two groups, whose pK_b values were redox-linked. Fitting of data employing Eqn. (1) allowed the pK_b values to be obtained for both the oxidized (${}^{ox}pK_{b1}$ and ${}^{ox}pK_{b2}$, see Scheme 1) and the reduced (${}^{red}pK_{b1}$ and ${}^{red}pK_{b2}$, see Scheme 1) forms of the enzyme; the values obtained from the fitting of experimental data are reported in Table 1. Both ionizable groups displayed a decrease in pK_b upon reduction; the first ionization decreased it from 5.95 ± 0.13 in the oxidized form to 5.13 ± 0.11 in the reduced form, and the second one decreased it from 9.39 ± 0.16 in the oxidized species to 8.17 ± 0.13 in the reduced species (Figure 2 and Table 1). Our previous work has demonstrated that over the same pH range three pH-dependent spectroscopic transitions (observed by optical electronic absorption) were detected for oxidized wt MnP [21], and the pK_a values [$= \log_{10} (1/K_a)$] were numbered by starting from that characterized by a lower pK_a value. In the present study the equation deals with the proton association equilibrium (expressed as pK_b), and protonating groups are then numbered starting from that characterized by the highest pK_b value [see Eqn. (1)]. One of the groups responsible for a spectroscopic transition observed previously (characterized by $pK_{a3} = 9.12 \pm 0.22$ [21]) displayed a pK_a value similar to that corresponding to the pK_{b1} value of the oxidized molecule in our experiments (see Table 1). However, each of the other two values obtained from the spectroscopic measurements [21] differs from the other pK_b value, affecting the redox properties. This becomes evident when our data on the pH-dependence of the redox potential are fitted with the pK_a values determined by Banci et al. [21] (see Figure 2, dashed line). Findings from the two studies are not necessarily in contradiction. Indeed, only those residues whose pK_b values vary upon change of the oxidation state can affect the proton-linked redox behaviour. Therefore the two residues determining the pH-dependence of the redox potential are not necessarily the same two (out of three possible residues) modulating the pH-dependence of the wt MnP spectroscopic properties [21].

At alkaline pH values the redox potential of wt MnP was very negative ($E_0 = -0.197 \pm 0.03$ V against a normal hydrogen electrode), and as the pH was lowered, the protonation of two residues made the redox potential progressively less negative. The value became positive at pH < 6.0, with an overall change of approx. 0.3 V between pH 10.5 and pH 4.5 (see Figure 2). These results indicate that the formation of a positive charge (or the disappearance of a negative one) in these two residues brings about a condition in the haem pocket which makes the reduction of the haem's iron more favourable.

The protonation of these groups also has an effect on the heterogeneous electron transfer reaction of the protein at the electrode surface, and thus with the external environment. The rate constant for the heterogenous electron transfer (k_s) was estimated at 25 °C under acidic [i.e. in 0.1 M sodium acetate, pH 5.0; $k_s = 2.8(\pm 0.3) \times 10^{-4}$ cm/s], neutral [i.e. in 0.1 M sodium phosphate, pH 7.0; $k_s = 9.0(\pm 1.0) \times 10^{-4}$ cm/s] and alkaline [i.e. in 0.1 M sodium carbonate, pH 9.2; $k_s = 1.9(\pm 0.3) \times 10^{-4}$ cm/s] conditions according to Nicholson [26]. The values of the rate constants were calculated by using $n = 1$ (i.e. the number of electrons involved in the electron transfer process) and a diffusion coefficient, D_0, of 8.0×10^{-8} cm^2/s, calculated by applying the equation reported previously [27]. The rate constant for the heterogeneous electron transfer in the singly protonated form at neutral pH was 4–5 times faster than in the unprotonated species at alkaline pH, and approx. 3 times faster than at acidic pH. This indicates that the protonation of the residue with the higher pK_b value results in a faster rate of electron exchange, whereas the second protonation event has an opposite effect, significantly reducing the reaction rate. The addition of 1 mM $MnCl_2$, which induces the complete formation of the MnP–Mn(II) complex did not change either the observed redox potential and/or the rate of electron transfer (results not shown). This observation is sig-

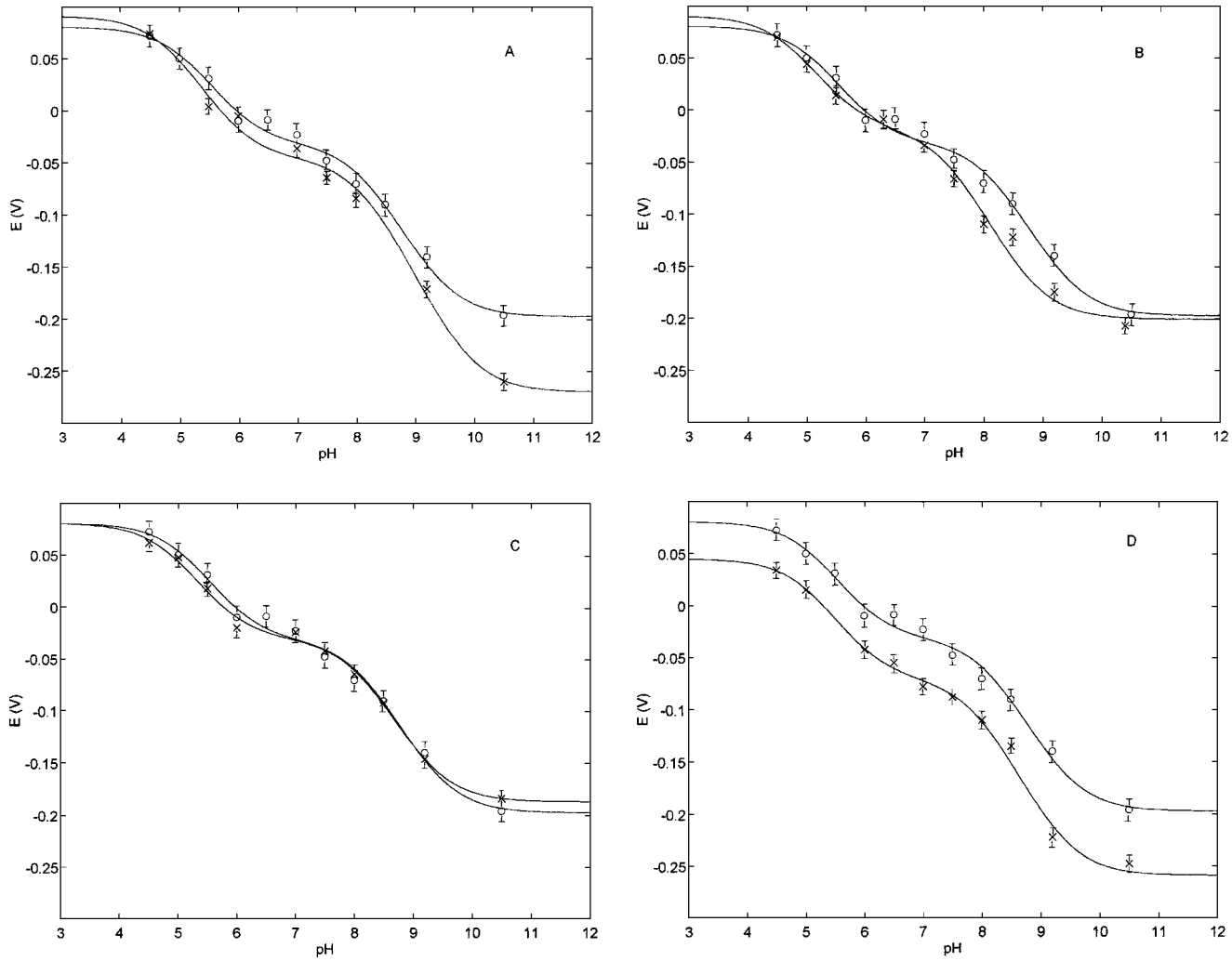

Figure 3 pH-dependence of the redox potential for mutants of MnP, namely D242E (A), D242S (B), F190V (C) and F190L (D)

Experimental points are the average of multiple measurements (at least three) and the standard deviations are reported. For clarity, in each panel the redox potentials of the mutant (×) are compared with the redox potential of wt MnP (○). Continuous lines were obtained by applying eqn. (1) with the parameters reported in Table 1. For further details see the text.

nificant, since it suggests that Mn(II), which is essential in the catalytic turnover of MnP as electron donor [4,5,28], does not appreciably affect the protonation equilibria of residues modulating the oxidation state of the haem's iron and the electron exchange rates of the protein with the bulk solvent.

For the purpose of identifying the residues involved in the proton-linked modulation of both the redox potential and the heterogeneous electron transfer, we have characterized mutants in the proximal pocket of MnP, namely at Asp^{242} and at Phe^{190}. These are the same mutants previously investigated [19,21]. Two of them (i.e. D242S and D242E) display a substitution of Asp^{242}, which is hydrogen-bonded to N_δ of the proximal His^{173} residue [6]. Mutations concern residues, which though able to form hydrogen-bonds with the proximal histidine, show either an increased length (i.e. glutamate) or the lack of a negative charge (i.e. serine). The other two mutants studied were at the Phe^{190} position (i.e. F190V and F190L), which had been substituted with other hydrophobic residues (i.e. valine or leucine) of smaller size than the aromatic ring of phenylalanine.

Figure 3 shows a comparison, as a function of pH, between the redox potential of wt MnP and those of the above mutants. It must be pointed out that results for these mutants at pH 7.0 are in agreement with those already reported [20].

The D242E mutation produced a more negative E_0 only at alkaline pH, and pK_b values were essentially the same as in the wt MnP, except for some variation of ${}^{ox}pK_{b1}$ (see Figure 3A and Table 1). This suggests that the increased residue length, resulting in a larger occupancy volume, has only a marginal effect on the functionally relevant proton-linked equilibria. However, the deprotonated form may impose some steric strain on the structural arrangement of the proximal side of the haem pocket, resulting in a less favourable reduction of the haem's iron. Conversely, the substitution of Asp^{242} with serine, which should produce a more dramatic change in the hydrogen-bonding network between residue 242 and His^{173}, had an effect on the first pK_b value (i.e. pK_{b1}; the residue which protonates at higher pH values); no variation was observed with either the second protonation value, pK_{a2}, or the redox potential, E_0, of the unprotonated molecule (see Figure 3B and Table 1). Thus the substitution of a negatively charged carboxy group of aspartate with the hydroxy group of serine resulted in a dramatic change in the pK_{b1} value, which turned out to be lower by approx. 0.6

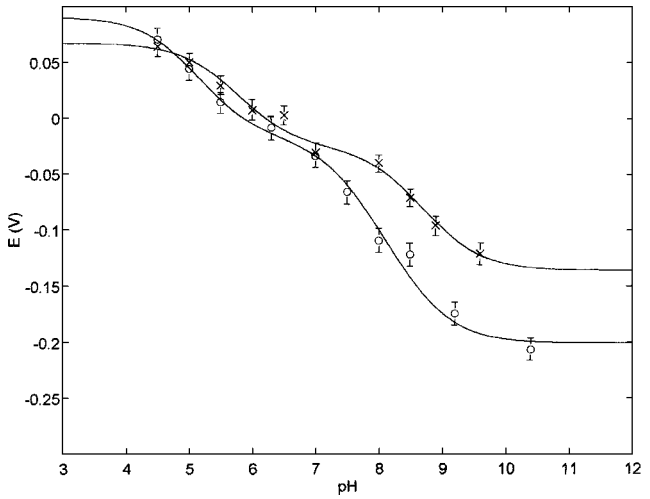

Figure 4 pH-dependence of the redox potential of the site-directed mutant D242S, employing different buffers (○) and only phosphate buffer (×)

Experimental points are the average of multiple measurements (at least three) and the standard deviations are reported. Continuous lines were obtained by applying eqn. (1) with the parameters reported in Table 1. For further details see the text.

pH unit with respect to that of wt MnP, in both the oxidized and reduced forms (see Table 1). These results suggest that the protonation of N_δ of the proximal His^{173} residue might be responsible for the proton-linked modulatory role on the redox properties of MnP. As a matter of fact the very close proximity of a negatively charged carboxy group (of Asp^{242}) may induce an increase in the pK_b of N_δ of the imidazole group of His^{173}, and this was observed in wt MnP (i.e. 9.39 ± 0.16 in the oxidized form and 8.17 ± 0.13 in the reduced form, see Table 1). The substitution of aspartate with glutamate induced only a limited change and only in the oxidized form (see Table 1). This may be due to the fact that the ionic character of the interaction with N_δ was unaffected by this mutation. The interaction between N_δ of His^{173} and the residue in position 242 may still be present in the D242S mutant. This would occur through hydrogen-bonding of the imidazole N_δ with the hydroxy group of serine. Consistent with this hypothesis, the lower pK_b value for the reduced form may be related to a decreased polarizing effect of Asp^{242} on N_δ of the proximal imidazole group. This may possibly be associated to a redox-linked conformational change of the proximal portion of the haem pocket, which affects the orientation and/or the distance between the residue at position 242 and N_δ of His^{173}. The very marginal effect, if any, on the second protonation event at acid pH values upon removal of the negative carboxy group in D242S (see Table 1) rules out any possible involvement of His^{173} in the modulation of this proton-linked process. It is important to point out that the heterogeneous electron transfer (k_s) at 25 °C in the D242S mutant displayed similar values to the wt MnP (i.e. $k_s = 4.0(\pm 0.3) \times 10^{-4}$ cm/s at pH 5.0 in 0.1 M sodium acetate, $k_s = 7.5(\pm 1.0) \times 10^{-4}$ cm/s at pH 7.0 in 0.1 M sodium phosphate and $k_s = 1.9(\pm 0.3) \times 10^{-4}$ cm/s at pH 9.2 in 0.1 M sodium carbonate), suggesting that the mutation does not appreciably affect this parameter.

On the other hand, it is very interesting to remark that the nature of the buffer affected the electrochemical behaviour of the D242S mutant, such that the value of E_0 at very alkaline pH values was much less negative in the presence of phosphate (see Figure 4 and Table 1). The presence of phosphate also caused an increase in the pK_{b1} values in both the oxidized and reduced forms of the D242S mutant relative to the wt species (see Table 1). The phosphate also affected the values of pK_{b2}, rendering them even higher than that observed in the wt enzyme (see Figure 4 and Table 1). In the previous spectroscopic characterization of these mutants it was found that phosphate facilitated the removal of the distal Ca^{2+}, which occurs with a pK_a intermediate between the pK_{b1} and pK_{b2} values. Apparently this effect was not detected in our measurements, because the pK_b value of this process is the same for the oxidized and the reduced state. Alternatively, it could occur that the protein experiences slightly different pK_b values in the oxidation states with and without distal Ca^{2+}. In any event, it appears that phosphate is able to modulate, in a specific way, the redox properties of MnP, a feature which cannot be attributed to only the negative charge on the phosphate, since the E_0 value and two pK_b values are all affected.

The functional effects of mutating Phe^{190} were less apparent. As shown in Figure 3(C), the F190V mutation did not induce a significant variation in either of the pK_a values of groups, which affect the redox properties of the enzyme (see Table 1). In the case of the F190L mutant (see Figure 3D), only the redox potential E_0 was affected (see Table 1). This result suggests that the longer aliphatic chain of leucine may induce, like in the case of the glutamyl residue in position 242 (see above), some steric disturbance to the conformation of the proximal His^{173} residue. This conformational change in turn renders the reduction process less favourable. However, in both mutants the substitution of Phe^{190} did not induce any effect on the proton-linked equilibria of the oxidized and reduced forms (see Table 1). This indicates that, as expected, this residue is not involved in interactions that regulate the pK_b of functionally relevant groups.

The 'acid' transition is completely unaffected by mutations at residues 242 and 190. This proton-linked feature is most likely attributed to a group that does not interact with the proximal side of the haem pocket of MnP, and its identification must await further investigation on additional mutants in different portions of the haem pocket.

In conclusion, the comparison between wt MnP and site-directed mutants provides a significant contribution to a deeper understanding of the system through the pH-dependence of redox potentials, allowing us to discriminate between effects on pK_b values from the intrinsic redox potential(s). This confirms the requirement for a complete investigation on the electron–proton coupling in order to afford a general description of the functional modulation mechanism in an electron carrier.

This work was partially supported by the programme Progetto Finalizzato Biotechnologie of the Italian CNR (contribution 99.00286.PF49), the Department of Energy grant DEFG02-87ER13690 to M.T., the Italian Ministero dell'Università e della Ricerca Scientifica e Tecnologica grant (MURST COFIN 9803184222) to M.C. and the European Union for the Network grant 'Foundations for controlling properties of haem proteins: structure/function relationships in archetypal systems and the development of an interdisciplinary methodology' (ERBFMRX CT 98 0218).

REFERENCES

1 Huynh, V. B. and Crawford, R. L. (1985) Novel extracellular enzymes (ligninases) of *Phanerochaete chrysosporium*. FEMS Microbiol. Lett. **28**, 119–123
2 Glenn, J. K. and Gold, M. H. (1985) Purification and characterization of an extracellular Mn(II)-dependent peroxidase from the lignin-degrading basidiomycete, *Phanerochaete chrysosporium*. Arch. Biochem. Biophys. **242**, 329–341
3 Glenn, J. K., Akileswaran, L. and Gold, M. H. (1986) Mn(II) oxidation is the principal function of the extracellular Mn-peroxidase from *Phanerochaete chrysosporium*. Arch. Biochem. Biophys. **251**, 688–696
4 Wariishi, H., Dunford, H. B., MacDonald, D. I. and Gold, M. H. (1989) Manganese peroxidase from the lignin-degrading basidiomycete *Phanerochaete chrysosporium*. Transient state kinetics and reaction mechanism. J. Biol. Chem. **264**, 3335–3340

5 Kuan, I.-C., Johnson, K. A. and Tien, M. (1993) Kinetic analysis of manganese peroxidase. The reaction with manganese complexes. J. Biol. Chem. **268**, 20064–20070
6 Sundaramoorthy, M., Kishi, K., Gold, M. H. and Poulos, T. L. (1994) The crystal structure of manganese peroxidase from *Phanerochaete chrysosporium* at 2.06-Å resolution. J. Biol. Chem. **269**, 32759–32767
7 Sundaramoorthy, M., Kishi, K., Gold, M. H. and Poulos, T. L. (1997) Crystal structures of substrate binding site mutants of manganese peroxidase. J. Biol. Chem. **272**, 17574–17580
8 Gajhede, M., Schuller, D. J., Henriksen, A., Smith, A. T. and Poulos, T. L. (1997) Crystal structure of horseradish peroxidase C at 2.15 Å resolution. Nat. Struct. Biol. **4**, 1032–1038
9 Poulos, T. L., Edwards, S. L., Wariishi, H. and Gold, M. H. (1993) Crystallographic refinement of lignin peroxidase at 2 Å. J. Biol. Chem. **268**, 4429–4440.
10 Petersen, J. W. F., Kadziola, A. and Larsen, S. (1994) Three-dimensional structure of a recombinant peroxidase from *Coprinus cinereus* at 2.6 Å resolution. FEBS Lett. **339**, 291–296
11 Finzel, B. C., Poulos, T. L. and Kraut, J. (1984) Crystal structure of yeast cytochrome c peroxidase refined at 1.7-Å resolution. J. Biol. Chem. **259**, 13027–13036
12 Wang, J., Mauro, J. M., Edwards, S. L., Oatley, S. J., Fishel, L. A., Ashford, V. A., Xuong, N. and Kraut, J. (1990) X-ray structures of recombinant yeast cytochrome c peroxidase and three heme-cleft mutants prepared by site-directed mutangenesis. Biochemistry **29**, 7160–7173
13 Banci, L., Bertini, I., Turano, P., Tien, M. and Kirk, T. K. (1991) Proton NMR investigation into the basis for the relatively high redox potential of lignin peroxidase. Proc. Natl. Acad. Sci. U.S.A. **88**, 6956–6960.
14 Edwards, S. L., Raag, R., Wariishi, H., Gold, M. H. and Poulos, T. L. (1993) Crystal structure of lignin peroxidase. Proc. Natl. Acad. Sci. U.S.A. **90**, 750–754
15 Goodin, D. B. and McRee, D. E. (1993) The Asp-his-Fe triad of cytochrome c peroxidase controls the reduction potential, electronic structure, and coupling of the tryptophan free radical to the heme. Biochemistry **32**, 3313–3324
16 Ferrer, J. C., Turano, P., Banci, L., Bertini, I., Morris, I. K., Smith, K. M., Smith, M. and Mauk, A. G. (1994) Active site coordination chemistry of the cytochrome c peroxidase Asp235Ala variant: spectroscopic and functional characterization. Biochemistry **33**, 7819–7829
17 Piontek, K., Glumoff, T. and Winterhalter, K. (1993) Low pH crystal structure of glycosylated lignin peroxidase from *Phanerochaete chrysosporium* at 2.5 Å resolution. FEBS Lett. **315**, 119–124
18 Poulos, T. L. and Kraut, J. (1980) A hypothetical model of the cytochrome c peroxidase: cytochrome c electron transfer complex. J. Biol. Chem. **255**, 10322–10330
19 Kishi, K., Hildebrand, D. P., Kusters-van Someren, M., Gettemy, J., Mauk, A. G. and Gold, M. H. (1997) Site-directed mutations at phenylalanine-190 of manganese peroxidase: effects on stability, function, and coordination. Biochemistry **36**, 4268–4277
20 Whitwam, R., Koduri, R. S., Natan, M. and Tien, M. (1999) Role of axial ligands in the reactivity of Mn peroxidase from *Phanerochaete chrysosporium*. Biochemistry **38**, 9608–9616
21 Banci, L., Bertini, I., Capannoli, C., Del Conte, R. and Tien, M. (1999) Spectroscopic characterization of active mutants of manganese peroxidase: mutations on the proximal side affect calcium binding of the distal side. Biochemistry **38**, 9617–9625
22 Whitwam, R. and Tien, M. (1996) Heterologous expression and reconstitution of fungal Mn peroxidase. Arch. Biochem. Biophys. **333**, 439–446
23 Millis, C. D., Cai, D., Stankovich, M. T. and Tien, M. (1989) Oxidation-reduction potentials and ionization states of extracellular peroxidases from the lignin-degrading fungus *Phanerochaete chrysosporium*. Biochemistry **28**, 8484–8489
24 Santucci, R., Ferri, T., Morpurgo, L., Savini, I. and Avigliano, L. (1998) Unmediated heterogeneous electron transfer reaction of ascorbate oxidase and laccase at a gold electrode. Biochem. J. **332**, 611–615
25 Nicholson, R. S. and Shain, I. (1964) Theory of stationary electrode polarography. Single scan and cyclic methods applied to reversible, irreversible and kinetic systems. Anal. Chem. **36**, 706–723
26 Nicholson, R. S. (1965) Theory and application of cyclic voltammetry for measurement of electrode reaction kinetics. Anal. Chem. **37**, 1315–1355
27 Bard, A. J. and Faulkner, L. R. (1980) In Electrochemical Methods: Fundamentals and Applications, pp. 230–231, John Wiley, New York
28 Wariishi, H., Akileswaran, L. and Gold, M. H. (1988) Manganese peroxidase from the basidiomycete *Phanerochaete chrysosporium*: spectral characterization of the oxidized states and the catalytic cycle. Biochemistry **27**, 5365–5370

Received 4 January 2000/23 March 2000; accepted 25 April 2000